Biomass Conversion and Biorefinery
https://doi.org/10.1007/s13399-024-05544-y

ORIGINAL ARTICLE

Biosynthesized copper oxide nanoparticles by *Psidium guajava* plants with antibacterial, antidiabetic, antioxidant, and photocatalytic capacity

Ankush Relhan[1] · Samriti Guleria[2] · Aparajita Bhasin[2] · Anis Mirza[1] · John L. Zhou[3]

Received: 28 November 2023 / Revised: 13 March 2024 / Accepted: 21 March 2024

Abstract

With an increasing focus on green technologies, this research aimed to synthesize copper oxide nanoparticles (CuO-NPs) using leaf extracts from Allahabad Safeda and Hisar Safeda for environmental and health protection. A range of concentrations of leaf extracts were employed in the synthesis of nanoparticles, utilizing 1–9% extract from Allahabad Safeda and 3–11% extract from Hisar Safeda. The synthesized CuO-NPs were characterized by UV–visible spectrophotometry, Dynamic light scattering, Fourier transform infrared spectroscopy, and Scanning electron microscope with energy-dispersive X-ray spectroscopy. CuO-NPs synthesized using 3% Allahabad Safeda extract and 5% Hisar Safeda extract exhibited a particle size of 15.88 nm and 14.05 nm, respectively. CuO-NPs synthesized with Allahabad Safeda extract exhibited superior antibacterial, antioxidant, antidiabetic, and photocatalytic properties. Their antibacterial tests demonstrated significant inhibition zones against *Staphylococcus aureus* (20.5 cm), *Streptococcus latis* (20.7 cm), *Escherichia coli* (19.5 cm), and *Pseudomonas aeruginosa* (19.7 mm). Additionally, CuO-NPs from Allahabad Safeda extract (70 µg/mL) exhibited 68.23% of scavenging activity against 2,2-diphenyl-1-picrylhydrazyl. Moreover, the same CuO-NPs at 100 µg/mL concentration showed 67.32% α-amylase inhibition and 75.18% α-glucosidase inhibition, confirming their antidiabetic activities. Furthermore, these nanoparticles demonstrated high performance in photocatalytic degradation, by degrading 82.31% methylene blue and 88.54% crystal violet within 150 min of UV irradiation. Overall, the findings highlight the feasibility of CuO-NPs synthesis using Allahabad Safeda extract and their potential applications in antibacterial treatment, combating diabetes, antioxidation, and environmentally friendly dye photodegradation process.

Keywords Antibacterial · Dye degradation · Diabetes management · Green synthesis · Nanoparticles · *Psidium guajava*

Highlights
- CuO nanoparticles were synthesized from leaf extracts of *Psidium guajava* plants.
- CuO nanoparticles exhibited a significant antioxidant activity.
- CuO nanoparticles were effective against gram-positive and gram-negative bacteria.
- CuO nanoparticles degraded cationic dyes under UV irradiation.

✉ Anis Mirza
Anis.19474@lpu.co.in

✉ John L. Zhou
junliang.zhou@uts.edu.au

Ankush Relhan
ankushrelhan5@gmail.com

Samriti Guleria
guleriasamriti@gmail.com

Aparajita Bhasin
jita.84@gmail.com

1 Introduction

Nanotechnology has become a revolutionary field of research, offering exciting opportunities to design and engineer materials with unique properties at the nanoscale [1, 2]. Nanoparticles possess distinctive qualities due to their size,

[1] Department of Horticulture, Lovely Professional University, 144411 Phagwara, India

[2] Department of Food Technology and Nutrition, Lovely Professional University, 144411 Phagwara, India

[3] School of Civil and Environmental Engineering, University of Technology Sydney, 15 Broadway, Ultimo, NSW 2007, Australia

Published online: 12 April 2024

shape, morphology, and large surface area which contribute to their potential applications [3, 4]. Conventional methods of synthesizing nanoparticles involve costly chemical and physical processes with the risk of causing environmental pollution, cellular toxicity, carcinogenicity, and ecological harm [5, 6]. Therefore, current scientific research has been geared towards less expensive and more eco-friendly synthesis approaches [7, 8]. Green nanoparticle synthesis has recently gained interest as a promising and sustainable alternative to conventional methods, to reduce the environmental impact of nanoparticle manufacturing [9, 10]. To synthesize nanoparticles, three essential requirements must be met: the selection of an environmentally friendly solvent, a suitable reducing agent, and a safe stabilizing substance [7, 11]. These factors are crucial for ensuring efficient and sustainable nanoparticle synthesis [12]. Green synthesis is generally carried out using medicinal plants, bacteria, fungi, herbs, spices, and hybrid materials [5, 13, 14]. These methods are more affordable, environmentally benign, and widely accessible [15].

In recent years, there has been a growing interest in using plant-based methods [16] to synthesize metal nanoparticles due to their wide range of potential applications. The characteristics of these nanomaterials are influenced by the biological and physicochemical properties of the plant-based synthesis process, which relies on specific phytoconstituents acting as reductants or stabilizers [17, 18]. Various plant extracts have been employed for the fabrication of metal nanoparticles such as gold, silver, copper, zinc, iron, nickel, and magnesium [19–23]. These nanoparticles have exhibited notable traits such as anti-diabetic, antibacterial, antiviral, anti-inflammatory, and antioxidant properties [21, 24–26]. Furthermore, such nanoparticles have shown catalytic activity because of their different nanostructure and large surface area, with potential application for effluent treatment of industrial dyes [14]. Among these, copper oxide nanoparticles (CuO-NPs) have gained substantial attention due to their versatile applications in medicine, environmental cleanup, and energy utilization [14, 27]. *Psidium guajava*, commonly known as the guava tree, is prevalent across Africa, Asia, Eastern Europe, and other regions. It belongs to the Magnoliophyta phylum, Magnoliopsida class, and Myrtaceae family, and is cultivated for its juicy fruits, medicinal attributes, and ornamental value. Guava leaves, in particular, contain a rich assortment of bioactive components, including phenolics, flavonoids, tannins, minerals, essential oils, ascorbic acid, proteins, and polysaccharides [28]. These constituents can serve effectively as both reductants and stabilizers in producing metal nanoparticles [29–31]. It is hypothesized that guava leaves can be used as a valuable material for the green synthesis of CuO-NPs with potential antibacterial, antidiabetic, antioxidation, and photocatalytic capabilities [32, 33]. The abundance and widespread availability of guava leaves make them an economical and sustainable resource for the eco-friendly synthesis of metal nanoparticles [34]. Incorporating plant extracts during the nanoparticle synthesis process not only enhances the physicochemical properties of the nanoparticles but also adds valuable bioactive components with potential health benefits [35, 36]. The increasing prevalence of chronic diseases, such as diabetes, has prompted the exploration of novel therapeutic strategies [37, 38]. In this context, nanoparticles have shown promise as potential therapeutic agents due to their unique physicochemical properties [24]. The nanoparticles derived from guava extract could offer a new avenue for addressing this global health challenge. Alongside their therapeutic potential, the antibacterial potential of copper oxide nanoparticles is of utmost importance in combating the growing threat of antibiotic resistance. By evaluating the efficacy of these nanoparticles against pathogenic microorganisms, we aim to shed light on their potential as an alternative antimicrobial agent. Additionally, the antioxidant capacity of copper oxide nanoparticles derived from guava leaf extracts is an essential aspect to explore, considering the rising interest in natural antioxidants for various health benefits [25, 30]. Moreover, the ability of these nanoparticles to scavenge free radicals and protect cells from oxidative stress-related diseases is assessed. Furthermore, the field of environmental remediation has benefitted from nanotechnology, with photocatalytic materials being employed to degrade harmful pollutants in water and air. CuO-NPs have demonstrated remarkable photocatalytic activity, especially in the degradation of organic dyes, which are persistent environmental contaminants [39, 40]. The objectives of this research were to synthesize copper oxide nanoparticles by the utilization of leaf extracts from two *Psidium guajava* varieties (Allahabad Safeda, Hisar Safeda), and to evaluate their capabilities in antibacterial properties, antioxidant activity, anti-diabetic effects, and photocatalytic degradation potential. By harnessing the green synthesis approach, this research contributes to the sustainable fabrication of CuO-NPs, while also exploring their multifaceted applications in healthcare and environmental protection.

2 Materials and methods

2.1 Chemicals, plants, and microbial culture

Leaf samples of Allahabad Safeda and Hisar Safeda were collected from the Agriculture field of Lovely Professional University, Phagwara, Punjab. Chemicals of AR grade such as copper sulfate ($CuSO_4 \cdot 5H_2O$), iodine crystal, sodium hydroxide, hydrochloric acid, nitric acid, 2,2-diphenyl-1-picrylhydrazyl (DPPH), and lipase were obtained from Sigma Aldrich, St. Louis, MO, USA. The antibiotic ampicillin,

muller hinton agar, and nutrient broth were procured from Hi-Media Pvt. Ltd., Mumbai, India. Bacterial cultures including *Staphylococcus aureus* (MTCC 3160), *Streptococcus lactis* (MTCC 5461), *Escherichia coli* (MTCC 443), and *Pseudomonas aeruginosa* (MTCC 424) were procured from the Microbial Type Culture Collection (MTCC), Institute of Microbial Technology, Chandigarh, India. Methylene blue (MB) and crystal violet (CV) were purchased from LOBA Chemie Pvt. Ltd. Mumbai, India, and Qualikems Fine Chem Pvt. Ltd. Vadodara, India, respectively. All chemicals used were of analytical reagent grade.

2.2 Preparation of plant leaf extracts

Leaf samples of *Psidium guajava* specifically Allahabad and Hisar Safeda varieties were collected and dried in an oven at 50 °C. Once dried, the samples were ground into a fine powder and stored in an airtight container for further use. To isolate the compounds from the dried *Psidium guajava* (varieties) leaf, a modified version of the method by Nagaraja et al. [41] was employed. In the extraction process, 5.0 g of the dried samples was mixed with 100 mL of double-distilled water. The mixture was then gently heated in a water bath at temperatures between 60 and 70 °C for 15 min. Then the mixture was cooled and thoroughly stirred with a magnetic stirrer for 20–30 min to enhance the extraction efficiency. To further separate the components, the resulting solutions were subjected to centrifugation at 10,000 × *g* rpm for 10 min. Then, the liquid extracts were filtered using Whatman No. 1 filter paper, with the filtrates being stored at 4 °C for further use.

2.3 Synthesis of copper oxide nanoparticles

A 10-mM solution of copper sulfate pentahydrate ($CuSO_4 \cdot 5H_2O$) was prepared, from which 25 mL was used to obtain the same concentration of copper sulfate in all experiments. To optimize the stabilization of copper oxide nanoparticles, different concentrations of Allahabad Safeda extract (1%, 3%, 5%, 7%, and 9%) and Hisar Safeda extract (3%, 5%, 7%, 9%, and 11%) were examined. The synthesis involved mixing the plant extracts with the copper sulfate solution while maintaining constant stirring for 20 min at 500 rpm and a temperature of 80 °C. During this process, a noticeable color change indicated the successful formation of copper nanoparticles (CuO-NPs) as described in the research by Ghosh et al. [13] and Gaber et al. [37].

2.4 Characterization of synthesized copper oxide nanoparticles

Initially, the synthesized copper oxide nanoparticles (CuO-NPs) were characterized for surface plasmon resonance using UV–visible spectroscopy (Evolution 201, Thermo Fischer Scientific India Pvt. Ltd, Mumbai). The UV–visible spectra of CuO-NPs were recorded in the scan mode within a wavelength range of 800–200 nm. Dynamic light scattering (DLS) was employed to determine the particle size of CuO-NPs dispersed in water. The zeta potential of the CuO-NPs with smaller particle sizes was evaluated using a Zeta potential analyzer (Zetasizer Nano ZS, Malvern Instruments Ltd., Malvern, WR14 1XZ, UK). To investigate the morphology of selected CuO-NPs, scanning electron microscopy (JEOL JSM-6510LV instrument from INCA, USA) was used. The elemental analysis of the nanoparticles was performed using energy-dispersive X-ray spectroscopy (RONTEC's EDS system Model QuanTax 200, USA.) Additionally, Fourier transform infrared spectroscopy (FTIR) analysis was conducted (Cary 630 Agilent) to identify the functional groups present in the CuO-NPs.

2.5 Application of synthesized copper oxide nanoparticles

2.5.1 Antimicrobial efficacy

The CuO-NPs were tested for their antimicrobial properties against four bacterial strains, two Gram-positive strains (*Staphylococcus aureus* and *Streptococcus lactis*) and two Gram-negative strains (*Escherichia coli* and *Pseudomonas aeruginosa*). The antibacterial activity of CuO-NPs was assessed using an agar well diffusion method [39]. The bacterial cultures were adjusted to a standard concentration of 0.5 McFarland, which is equivalent to a microbial suspension of 1.5×10^8 cfu/mL. For each experiment, Petri plates were filled with 25 mL of muller hinton agar medium and inoculated with the selected microorganisms using the spread plate method. After 30 min, the wells of 6 mm in diameter were carefully drilled into the agar plates and then filled with 100 µL of CuO-NPs reconstituted in DMSO. Negative control experiments were performed using DMSO, while chloramphenicol was used as a standard antibacterial agent (as positive control). Subsequently, all the plates were incubated at 37 °C for 24 h. To ensure accuracy, each experiment was repeated in triplicate. This methodology was followed to minimize errors and obtain reliable results regarding the antimicrobial activity of CuO-NPs against the tested bacterial strains.

2.5.2 Minimum inhibitory concentration and minimum bactericidal concentration

The broth dilution method was utilized to determine the minimum inhibitory concentration (MIC) values of CuO-NPs. In each test tube, 5 mL of nutrient broth was mixed with 50 µL of microorganisms and 500 µL of the CuO-NPs. The control contained only inoculated broth. Then the tubes were

incubated at 37 °C for 24 h, and the presence or absence of visible growth was noted. The MIC value was determined as the lowest concentration of the microalgae extract where no visible growth of bacteria was observed in the tubes. The turbidity of the tubes was visually examined both before and after incubation to confirm the MIC value. Once the MIC value was determined, 50-µL samples were taken from the tubes where no visible bacterial growth was observed. These samples were plated onto Muller Hinton agar and incubated at 37 °C for 24 h. After incubation, the agar plates were examined to assess the presence or absence of bacteria.

2.5.3 Antioxidant activity by DPPH scavenging assay

The DPPH radical scavenging assay was conducted to evaluate the antioxidant activity of green-synthesized CuO-NPs by using the protocol by Zafar et al. [42]. To prepare DPPH solution, 2.36 mg of DPPH was mixed with 100 mL of 95% methanol and various concentrations of nanoparticles (20–140 µg/mL) were prepared. In each of the test tubes, 3 mL of the prepared DPPH solution was taken, and then 100 µL respective nanoparticle concentration was added into the test tube. The reaction mixture in each test tube was vigorously shaken and then incubated for 30 min. After incubation, the resulting solutions were measured by UV–visible spectrophotometry at 517-nm wavelength. To establish a comparison, a control sample was prepared containing the same concentration of standard ascorbic acid as used for the test samples. Additionally, a blank sample was prepared using 95% methanol. The inhibition property of the nanoparticles was calculated using Eq. (1):

$$\%\ \text{inhibition} = \frac{A_{\text{control}} - A_{\text{test}}}{A_{\text{control}}} \times 100 \quad (1)$$

where A_{control} is the absorbance of the control reaction, and A_{test} is the absorbance in the presence of CuO-NPs derived from Allahabad and Hisar Safeda extract.

2.5.4 Antidiabetic assay

The anti-diabetic potential of CuO-NPs was evaluated using α-amylase and α-glucosidase inhibition assay reported by Zafar et al. [42].

α-Amylase inhibition assay The amylase inhibition activity was assessed using a method described by Khan et al. [43] with slight modification, in a 96-well microplate. Various concentrations of CuO-NPs (10–100 µg/mL) were prepared in DMSO. The synthesized CuO-NPs (20 µL) of different concentrations were added to the test well, followed by the addition of 25 µL of α-amylase solution (50 µg/mL), phosphate buffer (15 µL), and starch (40 µL). Then the mixture was incubated at 50℃ for 30 min. Next, 20 µL of 1 M HCl and 90 µL of iodine solution were loaded into each well. The mixture was then subjected to centrifugation at 3000 rpm for 5 min at 4 °C, from which the supernatant was collected for the optical density measurement at 540 nm in a spectrophotometer. In addition, acarbose was used as a positive control, which is known as an α-amylase inhibitor. Next, 20 µL of 1 M HCl and 90 µL of iodine solution were loaded into each well. The experiments were repeated three times for each concentration to ensure the accuracy. Amylase inhibitory activity was calculated by Eq. (2):

$$Amylase\ inhibition(\%) = \frac{Sample_{Abs} - Negative\ control_{Abs}}{Blank_{Abs} - Negantive\ control_{Abs}} \times 100 \quad (2)$$

where Abs represents the absorbance, and the concentration required to inhibit 50% of α-amylase (IC_{50}) was determined for acarbose and CuO-NPs derived from Allahabad Safeda and Hisar Safeda extracts.

α-Glucosidase inhibition assay A glucosidase inhibition assay was conducted to assess the α-glucosidase inhibitory potential of CuO-NPs using a modified procedure from Zafar et al. [42]. To dissolve α-glucosidase, 50 mL phosphate buffer (pH 6.8) and 100 mg of bovine serum albumin were mixed simultaneously. After 5 min, 490 µL of phosphate buffer (pH 6.8) and 250 µL of p-nitrophenyl-D-glucopyranoside (5 mM) were mixed and incubated at 37 °C for 15 min. Subsequently, ZnO-NPs were incubated with 250 µL of α-glucosidase for 15 min at 37 °C. The reaction was terminated using a 2 mL solution of Na_2CO_3 (200 mM), and the absorbance was measured at 400 nm. The experiment was repeated three times to minimize the error, with acarbose being used as a positive control. Glucosidase inhibition was calculated using Eq. (2), for amylase inhibitory activity.

2.5.5 Photocatalytic dye degradation

The effectiveness of CuO-NPs in the photodegrading of the dyes MB (10 mg/L) and CV (10 mg/L) was evaluated using an experimental procedure based on the method proposed by Guleria et al. [39] with some modifications. The dye solution's pH was kept at 8.5 using 0.1 N sodium hydroxide and hydrochloric acid solutions. The degradation of both dyes was examined under UV light (Philips, 150 W, wavelength = 200–280 nm), with the light source placed 20 cm away from the dye solution. To achieve absorption/desorption equilibrium, a suspension containing the dye and CuO-NPs was prepared and subjected to constant magnetic stirring at 150 rpm in dark conditions for 20–30 min. The experimental setup involved adding 25 mL of the dye solution and 1.0 mL of the CuO-NPs to a conical flask, which was continuously stirred. After the preparation of

the suspensions, they were exposed to UV light irradiation for photodegradation experiments. To monitor the degradation process, 2 mL of the sample was collected at specific time intervals (10, 20, 30, 40, 50, 60, 70, and 80 min) and centrifuged at 10,000 × *g* for 15 min to obtain the supernatant. The dye concentration in the supernatant was analyzed using UV–visible spectroscopy (Shimadzu 1700) based on the absorption spectra. The changes in the dye concentration over time were used to assess the efficiency of CuO-NPs in photodegrading MB and CV under UV light, by using Eq. (3):

$$\text{Dye degradation efficiency}(\%) = \frac{C_0 - C_t}{C_0} \times 100 \quad (3)$$

where C_0 and C_t were the initial and remaining dye concentrations (mg/L) of the aqueous solution at time 0 and t.

The kinetics of the photocatalytic decolorization rate of MB and CV tended to follow the pseudo-first-order kinetics, as given in Eq. (4):

$$ln\frac{C_0}{C_t} = kt \quad (4)$$

where k is the first-order rate constant (min^{-1}) and was calculated from the slope of ln (C_o/C_t) versus irradiation time.

2.5.6 Role of ROS in photocatalytic dye degradation

Experimental protocols by Xu et al. [44] and Guleria et al. [39] were utilized to assess the efficiency of reactive oxygen species (ROS) in degrading the dyes MB (10 mg/L) and CV (10 mg/L). The tests were carried out using the same photocatalytic reaction procedure that had been previously employed for CuO-NPs. The photocatalytic reaction procedure involved combining dye solution (25 mL), CuO-NPs (1 mL), and scavengers such as benzoquinone (BQ), ethylenediaminetetraacetic acid (EDTA), tertiary butyl alcohol (TBA), potassium iodide (KI), and silver nitrate ($AgNO_3$), which were then subjected to UV light irradiation for 80 min. Specifically, BQ was employed to neutralize the superoxide free radical ($O2^{-}$), while EDTA was utilized to counteract the formation of holes (h^+). In addition, TBA was introduced to eliminate the hydroxyl radical (·OH), and $AgNO_3$ was used to capture the free electrons.

3 Results and discussion

3.1 Synthesis and optimization of copper oxide nanoparticles by Psidium guajava extracts

CuO-NPs were successfully synthesized by reducing copper sulfate pentahydrate using aqueous extracts obtained from Allahabad Safeda and Hisar Safeda leaves. The nanoparticles were stabilized by varying concentrations of Allahabad Safeda extract (1%, 3%, 5%, 7%, and 9%) and Hisar Safeda extract (3%, 5%, 7%, 9%, and 11%) during the synthesis process. The completion of CuO-NP synthesis was confirmed by observing a color change from blue to brown (Fig. 1a), which indicated the occurrence of localized surface plasmon resonance in copper oxide nanoparticles [29, 30]. This phenomenon is a result of the sp-conduction band to the d-band transition of copper oxide nanoparticles [45]. The successful reduction of CuO-NPs with the plant extracts was supported by similar findings from previous studies [41, 46, 47]. The UV–visible spectra analysis was carried out in the wavelength of 800–200 nm (Fig. 1b, c).

3.2 Characterization of copper oxide nanoparticles

3.2.1 Particle size and zeta potential

The particle size results of CuO-NPs derived from Allahabad Safeda and Hisar Safeda are illustrated in Fig. 2. In this analysis, specific concentrations were chosen based on UV–visible spectra. For the CuO-NPs synthesized from Allahabad Safeda extract, different concentrations (3%, 5%, and 7%) were selected for particle size analysis. For CuO-NPs from Hisar Safeda, concentrations of 5%, 7%, and 9% were selected for particle size analysis. The particle size analysis revealed that CuO-NPs from Allahabad Safeda had sizes ranging between 20 and 50 nm (Fig. 2a, c), whereas CuO-NPs from Hisar Safeda showed sizes between 14 and 50 nm (Fig. 2d, f). Based on the smallest particle sizes in Table 1, one concentration from each CuO-NPs sample was chosen for further analysis. Specifically, 3% of Allahabad Safeda with a particle size of 15.88 nm and 7% of Hisar Safeda with a particle size of 14.05 nm were chosen. Additionally, an analysis of the zeta potential was performed on the selected concentrations (Fig. 2g, h).

3.2.2 Scanning electron microscopy

The morphology and structural characterization of plant-synthesized CuO-NPs nanoparticles were examined using SEM. Figure 3a and d represent the SEM images of the CuO-NPs derived from Allahabad Safeda and Hisar Safeda extracts. The SEM micrographs revealed the presence of CuO-NPs with varying diameters, indicating a polydisperse distribution. These nanoparticles exhibited a variety of shapes, irregular surfaces, and small structures with uneven edges. This diversity in morphology can be attributed to the synthesis process involving the plant extracts. As previously mentioned, the average particle size remained minimal due to the low concentration of copper sulfate, which promoted electrostatic stabilization and prevented aggregation. In

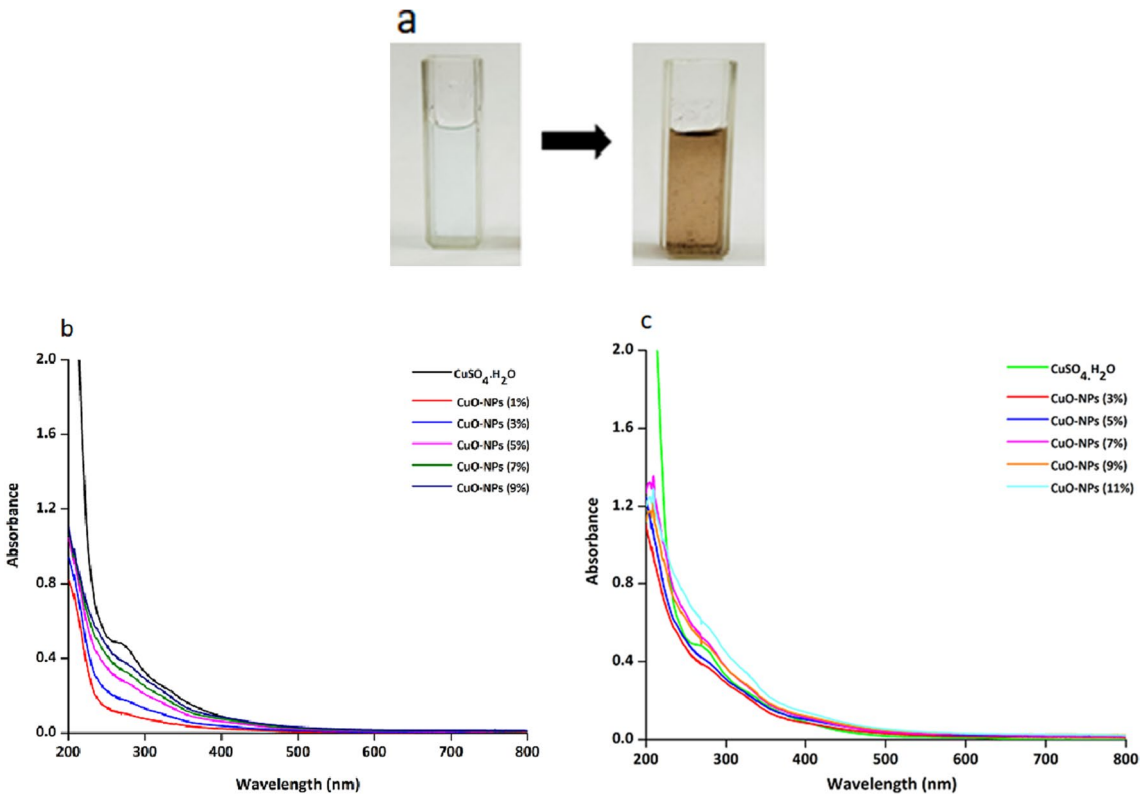

Fig. 1 **a** Visible confirmation of CuO-NPs, and UV–visible spectra of CuO-NPs derived from **b** Allahabad Safeda extract (1–9%) and **c** Hisar Safeda extract (3–11%)

addition, the composition of the CuO-NPs synthesized using the green method was analyzed through energy-dispersive X-ray (EDX) analysis and the EDS graph with KeV on the *x*-axis and peak intensity on the *y*-axis. As shown in Fig. 3b and e, the EDX spectra show the percentage composition of elements, with major elemental peaks observed at 1 keV, 8 keV, and 9 keV for CuO-NPs derived from Allahabad Safeda extract and at 0.95 keV for CuO-NPs derived from Hisar Safeda extract, which indicated the presence of copper. Additionally, minor peaks corresponding to the biomolecules used for capping the CuO-NPs were also detected.

3.2.3 Fourier transform infrared spectroscopy

FTIR was used to identify the functional groups present in plant extracts that contribute to the stabilization of CuO-NPs. The FTIR spectra of cupric sulfate solution, extracts from Allahabad Safeda and Hisar Safeda plants, and the resulting copper oxide nanoparticles obtained from these extracts are shown in Fig. 3c and f. The FTIR spectra of cupric sulfate pentahydrate exhibited prominent peaks at 3328.55 cm^{-1}, 2112.10 cm^{-1}, 1639 cm^{-1}, and 586.25 cm^{-1}, which correspond to O–H stretching, H-bonded interactions, C = C stretching, and Cu–O stretching vibrations, respectively [46]. In contrast, the spectra of Allahabad Safeda and Hisar Safeda extracts revealed multiple peaks at 3333, 3226, 230, 1633, 1075, 589, and 2223 cm^{-1}, which signify the presence of diverse bioactive phenolic compounds within the extracts [21], whereas CuO-NPs derived from Allahabad Safeda extract showed a band at 3272 cm^{-1} indicating O–H stretching and H-bonding [41]. Additional bands at 2119 cm^{-1} were attributed to C–H stretching and symmetric stretching, while the peaks at 1068 cm^{-1} and 872 cm^{-1} indicated C–O stretching, and C–Cl stretching, respectively [46]. In comparison, CuO-NPs synthesized from Hisar Safeda extract displayed a peak at 2115 cm^{-1}, attributed to C = C stretching. Additional bands at 1199 cm^{-1}, 1604 cm^{-1}, and 1648 cm^{-1} also indicated C = C stretching [48]. An interesting observation was the presence of a band at 1431 cm^{-1}, which was absent in the spectra of synthesized copper oxide nanoparticles. This band was assigned to N–H bending and stretching, possibly originating from an amide group, which may be responsible for the reduction of CuO-NPs. Additionally, a band at 698 cm^{-1} was identified, associated with C–Cl stretching from an alkyl halide group, which also played a role in the reduction of CuO-NPs. These functional groups are formed through interactions between the plant extracts and CuO-NPs, contributing to the production of plant-synthesized CuO-NPs. This finding is consistent with the work of Islam et al. [49], who

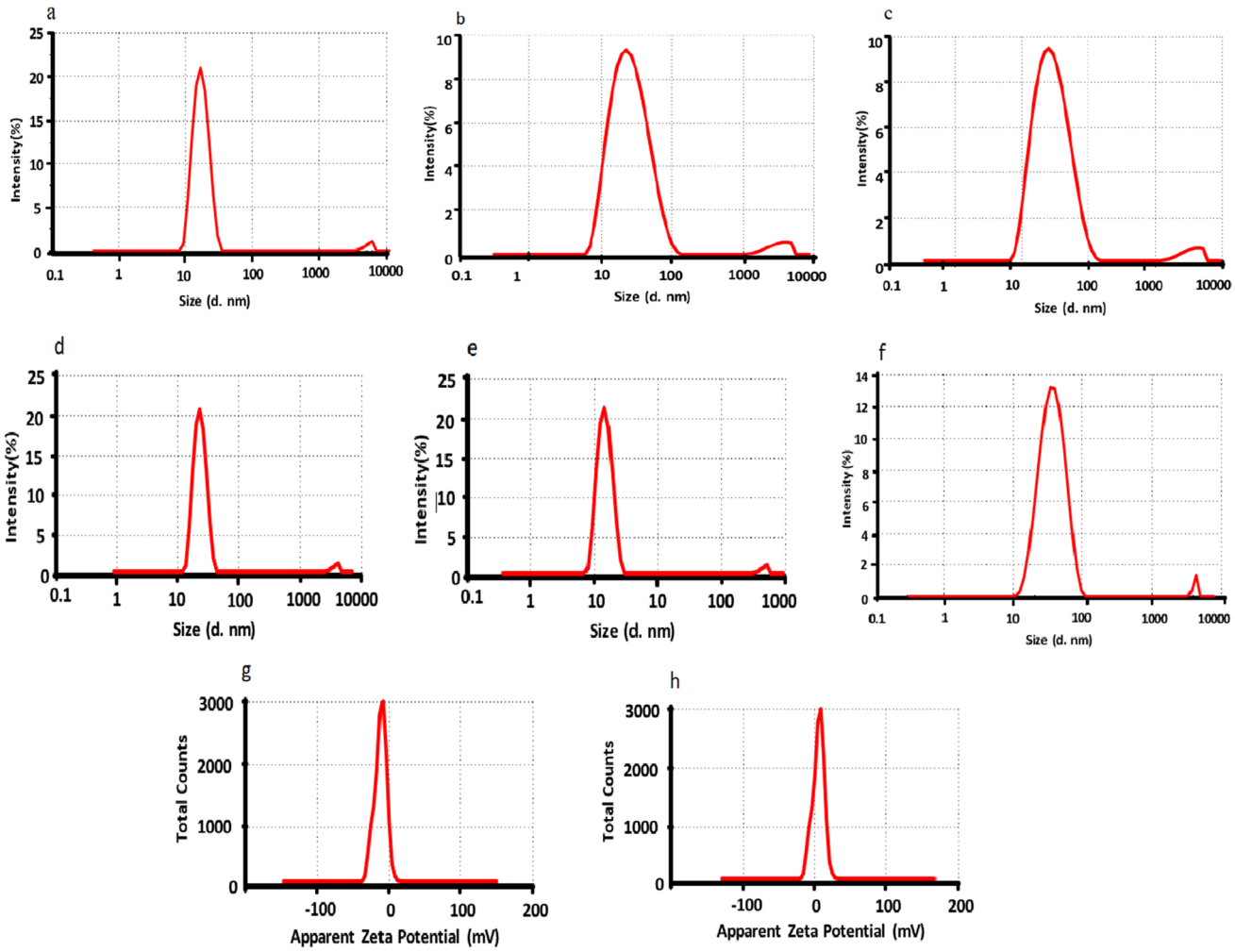

Fig. 2 The average particle size of CuO-NPs synthesized by using **a** Allahabad Safeda extract of 3%, **b** 5%, and **c** 9%; and **d** Hisar Safeda extract of 5%, **e** 7%, and **f** 9%. The zeta potential of CuO-NPs with the least particle size was synthesized using **g** 3% of Allahabad Safeda and **h** 7% of Hisar Safeda extracts

Table 1 The particle size of CuO-NPs derived from different leaf extracts

Plant extracts for the synthesis of CuO-NPs	Concentration of extract used (%)	Particle size of CuO-NPs (nm)
Allahabad Safeda	3	15.88 ± 6.46
	5	20.28 ± 7.86
	7	26.34 ± 8.24
Hisar Safeda	5	17.69 ± 5.42
	7	14.05 ± 4.57
	9	48.86 ± 17.23

identified hydroxyl, alkyne, and alkene groups in plants that were involved in copper nanoparticle synthesis. The elemental analysis further confirmed the presence of significant copper content alongside minor functional compounds.

3.3 Application of synthesized copper oxide nanoparticles

The efficiency of green synthesized CuO-NPs in antimicrobial activity, antioxidant potential, antidiabetic properties, and photocatalytic dye reduction was comprehensively assessed.

3.3.1 Antimicrobial activity

The antibacterial effectiveness of CuO-NPs against various pathogenic bacteria was determined, and the diameter of the inhibition zone around each well is presented in Fig. 4a. When comparing CuO-NPs synthesized from different *Psidium guajava* (Allahabad Safeda and Hisar Safeda) varieties, the CuO-NPs obtained from Hisar Safeda extract exhibited a significantly lower zone of inhibition compared to CuO-NPs

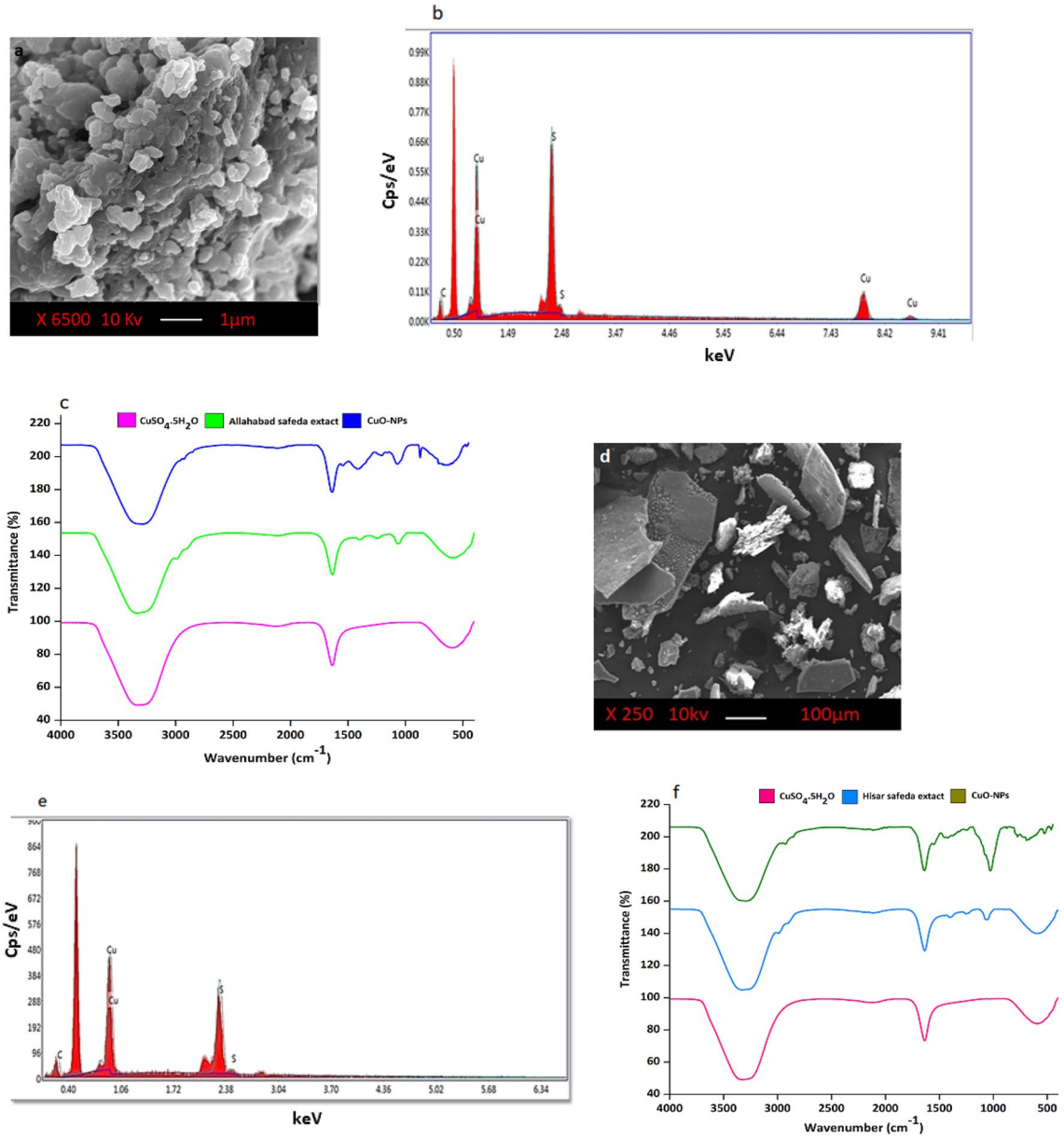

Fig. 3 Characterization of CuO-NPs derived from Allahabad Safeda extract by **a** scanning electron microscopy, **b** EDX, and **c** FTIR analysis; and CuO-NPs from Hisar Safeda extract by **d** scanning electron microscopy, **e** EDX, and **f** FTIR analysis

synthesized from Allahabad Safeda extract. Particularly, CuO-NPs derived from Allahabad Safeda extract showed a higher zone of inhibition for *Staphylococcus aureus* (20.5 mm), *Streptococcus lactis* (20.7 mm), *Escherichia coli* (19.5 mm), and *Pseudomonas aeruginosa* (19.7 mm). In addition, in the positive control group, CuO-NPs synthesized from extracts of both plants exhibited a significant zone of inhibition (24–25 mm) against all the tested bacterial strains. Based on the findings, it can be inferred that CuO-NPs derived from Allahabad Safeda extract are more promising as a potential source of antimicrobial compounds than CuO-NPs derived from Hisar Safeda extract. It is reported that *Lysiloma acapulcensise* extract-derived Ag-NPs showed a high antibacterial effect against *E.coli* with the inhibition zone 18.0 ± 1.3 mm, 16.0 ± 1.0 mm for *Staphylococcus aureus* [7]. Furthermore, a promising wide-spectrum antimicrobial activity was exhibited by graphene oxide from *Ziziphus spinna-cristi* extracts [50]. CuO-NPs derived from *Mangifera indica* aqueous extract showed effective antibacterial activities toward both *E. coli* and *S. aureus* strains [11]. Moreover, *Curcuma longa*–derived copper oxide nanoparticles exhibited effective antimicrobial potential against *P. aeuroginosa* and *P. vulgaris* [27]. Furthermore, Ullah et al. [51] demonstrated that gold nanoparticles synthesized

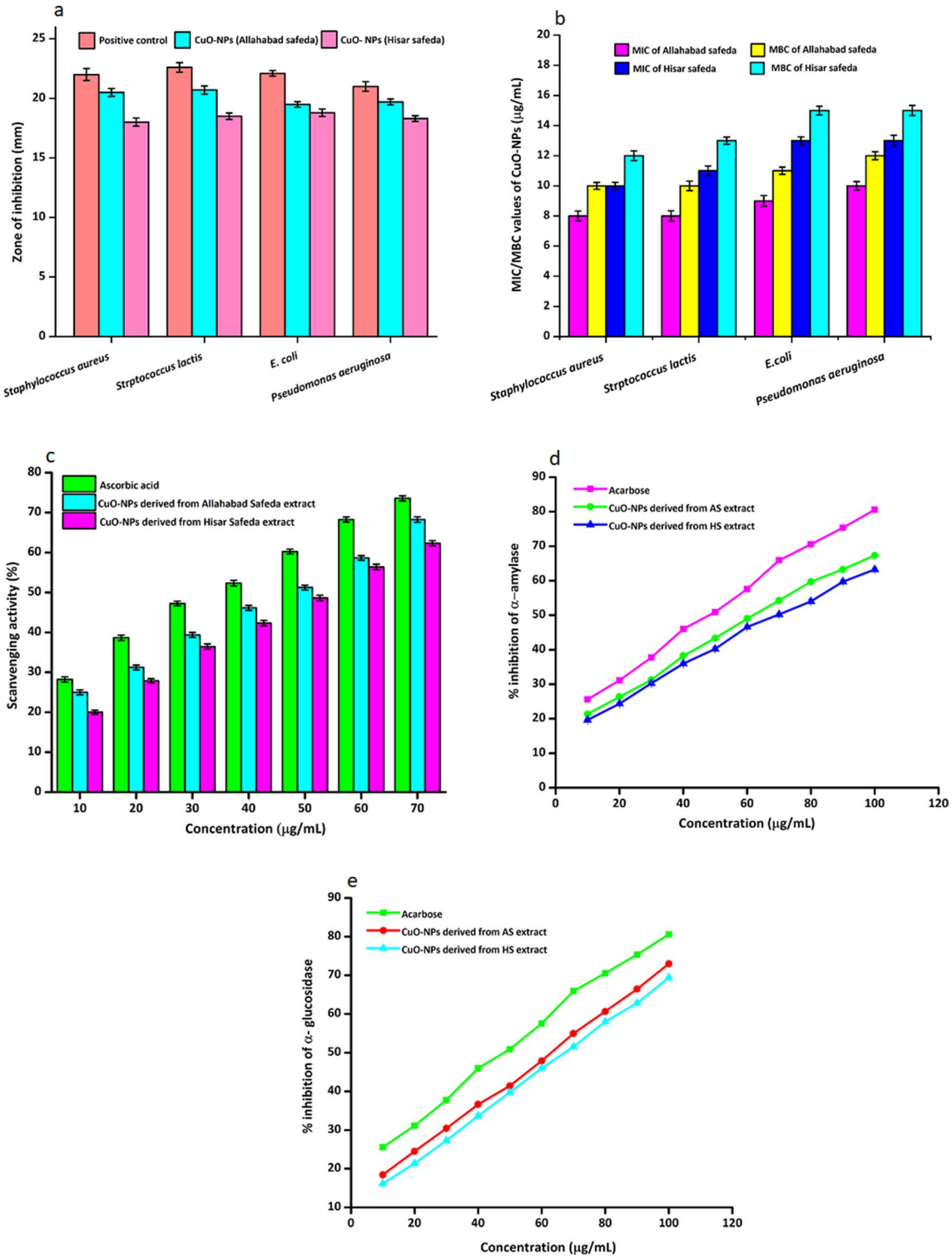

Fig. 4 **a** Zone of inhibition, **b** minimum inhibitory concentration (MIC) and minimum bactericidal concentrations (MBC), **c** DPPH scavenging activity, and **d** amylase inhibitory effects of CuO-NPs derived from Allahabad Safeda and Hisar Safeda extracts

using *Euphorbia wallichii* shoot extract possessed potent antibacterial activity against a range of common pathogens, including *Escherichia coli*, *Staphylococcus aureus*, *Bacillus pumilus*, *Pseudomonas aeruginosa*, and *Klebsiella pneumoniae*. Moreover, Al-Radadi et al. [2] demonstrated the antibacterial potential of silver nanoparticles mediated by using

Spirogyra hyalina extract. In addition, according to several studies conducted by Caroling et al. [52], Ntoumba et al. [53], Sathiyavimal et al. [54], Imran et al. [16], Hassan et al. [49], and Dinh et al. [21], *Psidium guajava* extract contains various active metabolites such as phenolics, flavonoids, tannins, minerals, essential oils, ascorbic acid, proteins, and polysaccharides that inhibit the bacterial growth. CuO-NPs derived from Allahabad Safeda extract exhibited higher antimicrobial activity due to their well-developed chemical stability surface chemistry, allowing effective interaction with the microorganisms. Their smaller size enhances their ability to interact with microorganisms and enhance their antimicrobial properties. CuO-NPs target the outer membrane, leading to structural changes, degradation, and cell lysis [39]. They also hinder microorganisms' DNA replication, resulting in inhibitory effects [55]. Moreover, their positive charge enables electrostatic interactions with the negatively charged cell membranes of microorganisms, leading to their death. In addition, CuO-NPs derived from herbal extracts produce ROS, which can damage the DNA and cell membranes of microbes, inhibiting their growth [56]. Furthermore, active metabolites from CuO-NPs can disrupt the quorum-sensing systems of bacteria, preventing them from causing infections. CuO-NPs release copper cations that can attach electrostatically to the cell walls of bacteria, and penetrate the surface of the bacterial membrane, further contributing to their bactericidal activity [57, 58]. In summary, CuO-NPs derived from plant extracts possess multiple antimicrobial mechanisms, including physical interactions with cell membranes, inhibition of DNA replication, generation of ROS, and interference with bacterial quorum sensing. These properties make CuO-NPs effective in defending against pathogenic microorganisms [3, 9, 13, 22].

3.3.2 MIC and MBC values

The MIC is the lowest concentration of test compounds that inhibit the visible growth of microorganisms, whereas minimum bactericidal concentration (MBC) is defined as the lowest concentration of antimicrobial agent that causes a 99.9% reduction in the bacterial population. The results (Fig. 4b) show the MIC and MBC values of CuO-NPs synthesized from the extracts of two different *Psidium guajava* varieties (Allahabad Safeda, Hisar Safeda). According to the findings, CuO-NPs derived from Allahabad Safeda extract exhibited lower MIC and MBC values than those from Hisar Safeda extracts. Especially, the MIC values of CuO-NPs from Allahabad Safeda extract against *S. aureus*, *S. lactis*, *E. coli*, and *P. aeruginosa* were found to be 8, 8, 9, and 10 µg/mL respectively. Correspondingly, the MBC values for these bacteria were 10, 10, 11, and 12 µg/mL respectively. In contrast, MIC values of CuO-NPs derived from Hisar Safeda extract were found to be 10, 11, 13, and 13 µg/mL against *S. aureus*, *S. lactis*, *E. coli*, and *P. aeruginosa*, respectively. Additionally, MBC values for these bacteria were determined to be 12 µg/mL, 13 µg/mL, 15 µg/mL, and 15 µg/mL, respectively.

3.3.3 DPPH scavenging assay

The DPPH assay was conducted to assess the scavenging properties of CuO-NPs synthesized using a green method. The ability of CuO-NPs to act as hydrogen donors is responsible for their scavenging activities. Figure 4c illustrates the results of different concentrations of CuO-NPs, along with ascorbic acid as a positive control. Both CuO-NPs and ascorbic acid demonstrated significant inhibition of DPPH radicals. In this study, CuO-NPs derived from Allahabad Safeda extract exhibited the highest inhibition of 68.23% at a concentration of 70 µg/mL, while CuO-NPs from Hisar Safeda showed inhibition of 62.32% at the same concentration. The positive control, ascorbic acid, showed the highest inhibition of 73.55% at the same concentration. These results suggest that the scavenging activity of CuO-NPs increases with higher sample concentrations, which is consistent with previous findings that higher concentrations of samples lead to increased inhibitory activity [59]. This can be attributed to the presence of phytoconstituents in the crude extract, contributing to the higher antioxidant activity of the CuO-NPs. Numerous researchers have explored the potential of nanoparticles derived from natural sources. Khan et al. [43] demonstrated that cobalt oxide and magnesium oxide nanoparticles synthesized using *Hibiscus rosa sinensis* extracts exhibited promising antioxidant activity. Similarly, Xu et al. [44] reported excellent antioxidant potential from nanoparticles derived from *Psidium guajava*. Additionally, Shah et al. [60] and Kokilananthan et al. [61] highlighted the inhibitory activity of gold nanoparticles synthesized from *Sageretia thea* leaf extract. These studies collectively point towards the potential of naturally derived nanoparticles as antioxidants, opening avenues for further research and development in this promising field. For scavenging the DPPH radicals, the CuO-NPs exhibit three primary mechanisms such as electron transfer, hydrogen atom transfer, and metal-ion complexation. In the electron transfer mechanism, CuO-NPs can act as electron donors for DPPH radicals, causing their inactivation and decolorization [27]. This process is often associated with the presence of Cu(I) ions on the nanoparticle surface. In the case of hydrogen atom transfer, specific surface hydroxyl groups on CuO-NPs can donate hydrogen atoms to DPPH radicals, thereby quenching their free radical character. Additionally, in metal-ion complexation, Cu(II) ions on the nanoparticle surface can form complexes with DPPH radicals, thereby stabilizing and reducing their radical activity, as reported by Peddi et al. [62], Luque et al. [63], Kaningini [45], and Abdullah et al. [1].

3.3.4 α-Amylase and α-glucosidase inhibition assay

The results of α-amylase and α-glucosidase inhibition assays for different concentrations of CuO-NPs synthesized from Allahabad Safeda, Hisar Safeda extract, and acarbose are provided in Fig. 4d and e, and Tables 2 and 3. In the α-amylase inhibition assay, acarbose of 100 µg/mL showed 77.98% inhibitory effects with an IC_{50} value of 55.32 µg/mL. CuO-NPs derived from Allahabad Safeda exhibited an inhibition effect of 67.32% at a concentration of 100 µg/mL, with an IC_{50} value of 65.21 µg/mL. Such an inhibition is more significant ($P < 0.005$) than by CuO-NPs from Hisar Safeda which showed 63.25% inhibition and IC_{50} of 70.26 µg/mL. In the α-glucosidase inhibition assay, acarbose demonstrated a notable inhibitory effect, with 80.56% inhibition at a concentration of 100 µg/mL and an IC_{50} value of 53.32 µg/mL. CuO-NPs from Allahabad Safeda exhibited a higher inhibition effect (75.18% inhibition at 100 µg/mL and IC_{50} value of 60.59 µg/mL) than CuO-NPs from Hisar Safeda (71.38% inhibition and an IC_{50} of 65.62 µg/mL). These results indicate the promising inhibitory potential of CuO-NPs from both Safeda extracts against α-amylase and α-glucosidase activity. Recent research suggests nanoparticles hold promise in combating diabetes. Studies by Faisal et al. [14] and Al-Radadi et al. [2] demonstrated the anti-diabetic potential of zinc oxide nanoparticles (ZnO-NPs). Radadi et al. explored ZnO-NPs specifically derived from Zingiber officinale (ginger). Zafar et al. [42] reported iron oxide nanoparticles (FeO-NPs) derived from Enterobacter biomass showing anti-diabetic activity. Recently, diabetes mellitus has become the most common endocrine disorder in India, attributed to people's lifestyle and genetic disorders. This condition causes morbidity and mortality globally, accompanied by a range of associated complications [24, 59, 63]. The digestive enzymes like α-amylase and α-glucosidase can hydrolyze starch, which is involved in postprandial hyperglycemia [31]. The inhibition of these two enzymes by nanomaterials can reduce the release and

Table 2 α-Amylase inhibitory effects of acarbose and CuO-NPs derived from Allahabad Safeda and Hisar Safeda extracts

Concentration (µg/mL)	%Inhibition of α-amylase					
	Acarbose	IC_{50} value (µg/mL)	CuO-NPs derived from Allahabad Safeda	IC_{50} value (µg/mL)	CuO-NPs derived from Hisar Safeda	IC_{50} value (µg/mL)
10	24.56 ± 0.32	53.32	21.35 ± 0.24	65.21	19.63 ± 0.25	70.26
20	29.12 ± 0.51		26.32 ± 054		24.36 ± 0.34	
30	36.63 ± 0.21		31.24 ± 0.47		30.23 ± 0.14	
40	42.52 ± 0.24		38.23 ± 0.36		35.95 ± 0.47	
50	49.96 ± 0.47		43.32 ± 0.42		40.21 ± 0.54	
60	55.36 ± 0.54		48.99 ± 0.27		46.59 ± 0.37	
70	60.59 ± 0.24		54.23 ± 0.24		50.21 ± 0.28	
80	66.23 ± 0.48		59.68 ± 0.34		53.98 ± 0.37	
90	71.35 ± 0.57		63.23 ± 0.48		59.69 ± 0.24	
100	77.98 ± 0.14		67.32 ± 0.26		63.25 ± 0.29	

Table 3 α-Glucosidase inhibitory effects of acarbose and CuO-NPs derived from Allahabad Safeda and Hisar Safeda extracts

Concentration (µg/mL)	%Inhibition of α-glucosidase					
	Acarbose	IC_{50} value (µg/mL)	CuO-NPs derived from Allahabad Safeda	IC_{50} value (µg/mL)	CuO-NPs derived from Hisar Safeda	IC_{50} value (µg/mL)
10	25.56 ± 0.32	53.32	18.43 ± 0.32	60.59	16.63 ± 0.25	65.62
20	30.12 ± 0.51		25.52 ± 0.57		22.36 ± 0.34	
30	36.73 ± 0.21		32.43 ± 0.52		30.29 ± 0.14	
40	41.98 ± 0.24		38.93 ± 0.46		36.65 ± 0.47	
50	49.89 ± 0.47		46.42 ± 0.54		43.71 ± 0.54	
60	57.56 ± 0.54		50.89 ± 0.34		47.99 ± 0.37	
70	65.89 ± 0.24		58.98 ± 0.52		55.51 ± 0.28	
80	70.53 ± 0.48		62.66 ± 0.35		60.98 ± 0.37	
90	75.35 ± 0.57		69.44 ± 0.47		65.79 ± 0.24	
100	80.56 ± 0.14		75.18 ± 0.36		71.38 ± 0.29	

absorption of glucose in the small intestine, leading to antidiabetic activity [64]. The main mechanisms shown by the extracts are to decrease the digestion of glucose and carbohydrates, which targets reducing postprandial hyperglycemia, and to reduce the hydrolysis process in the enzymatic reaction of carbohydrate complexes [65].

3.3.5 Photocatalytic dye degradation

Once the CuO-NPs were synthesized using extracts from two different guava varieties, their photodegradation of MB and CV under the irradiation of UV light was evaluated. The spectral changes were observed for MB at various time intervals while being irradiated by the UV light (Fig. 5a, b). It was observed that CuO-NPs derived from Allahabad Safeda extract were more effective in degrading MB (82.31%) compared to CuO-NPs synthesized from the extracts of Hisar Safeda (72.69%), at the end of 150 min (Fig. 5c). The findings highlighted the superior photocatalytic activity of CuO-NPs derived from Allahabad Safeda extract under UV irradiation. To further assess the impact of the CuO-NPs, a controlled study without CuO-NPs was also performed under UV irradiation, where no obvious spectral changes were observed, indicating very limited dye degradation. In addition, the photodegradation efficiency was only 17% under irradiation of light at the end of 150 min. Furthermore, the photodegradation kinetics results showed that the degradation rate under CuO-NPs was relatively constant over time. The kinetics of the MB photocatalytic decolorization were fitted to the Langmuirnear–Hinshelwood model, suggesting that the use of CuO-NPs could be effective for the efficient degradation of dyes under the irradiation of UV light. The photodegradation kinetics parameters for dye removal are shown in Table 4.

Similar to MB, CV photodegradation under UV light was examined (Fig. 5d, e). CuO-NPs derived from Allahabad Safeda extract showed a higher photodegradation of CV than from Hisar Safeda extract (Fig. 5g). Based on the UV photodegradation kinetics, a higher removal of CV was obtained by CuO-NPs from Allahabad Safeda extract (88.54%) than by CuO-NPs from Hisar Safeda extract (76.78%) at the end of experiments (Fig. 5f). Furthermore, a controlled study without CuO-NPs was also performed under UV irradiation, showing minimal spectral changes and little dye degradation. Specifically, the photodegradation efficiency was only 16% after 150 min of light irradiation. The results show that the degradation rate under CuO-NPs was relatively constant over time. The kinetics of the CV photocatalytic removal also followed the Langmuirnear–Hinshelwood model, as shown in Table 3.

The dye degradation potential of various metal oxide nanoparticles synthesized using diverse plant extracts has been reported. The findings of this study are in line with Muthukumar and Matheswaran [46] who demonstrated the potential of iron oxide nanoparticles derived from *Amaranthus spinosus* leaf extract, resulting in 75% and 69% decolorization of methyl orange and MB respectively. Faisal et al. [28] synthesized ZnO-NPs which showed 88% of MB degradation within 140 min. Chandraker et al. [7] utilized *Ageratum houstonianum* leaf extract to deriv CuO-NPs and evaluated their degradation potential against azo dye and congo red dye. Moreover, Vishnu et al. [66] investigated the potential of a cobalt-doped cadmium ferrite nanoparticle for the degradation of MB resulting in 60% degradation after 2 h. In addition, Oliveira Gaber et al. [67], Sibhatu et al. [65], Selvam et al. and Kumar et al. [68] have also investigated the potential of different nanoparticles in the degradation of various dyes, showing effective dye degradation.

3.3.6 Mechanisms of dye degradation by CuO-NPs

The dye degradation process on the surface of CuO-NPs initiates with the absorption of a photon with energy equal to or greater than the band-gap energy of the CuO-NPs, as described by Rezaie et al. [69]. This photon absorption leads to the excitation of an electron (e^-) from the valence band to the conduction band of CuO-NPs, resulting in the generation of a hole (h^+) in the valence band. As a result of the generation of electrons and holes, reduction–oxidation reactions take place on the surface of CuO-NPs [70]. In the reduction reaction, the electrons in the conduction band can either reduce the dye or react with electron acceptors, such as O_2 molecules adsorbed on Cu(II) surface or dissolved in water, which results in the reduction of O_2 to superoxide radical anion ($O_2^{-\cdot}$). In the oxidation reaction, the holes in the valence band can oxidize organic molecules, forming R^+ species, or react with OH^- ions or water, oxidizing them into hydroxyl radicals (OH·) [71]. These highly reactive species, including peroxide radicals, play a crucial role in the photo-decolorization of organic substrates such as dyes on CuO-NPs surfaces [72]. The resulting OH· radicals are an extremely potent oxidizing agent and can efficiently oxidize many azo dyes, ultimately converting them into mineral end-products. Consequently, the relevant reactions occurring at the CuO surface responsible for the decomposition of dyes can be expressed as follows, in alignment with the findings of Wardani et al. [73], Rezaie et al. [69], Faisal et al. [28], and Guleria et al. [39].

Reduction reaction:

$$e^-(\text{conduction band}) + O_2 \rightarrow O_2^{-\cdot}(\text{superoxide radical anion})$$

Oxidation reaction:

$$h^+(\text{valence band}) + \text{Organic molecule} \rightarrow R^+(\text{oxidized product})$$

$$h^+(\text{valence band}) + OH^- \text{or } H_2O \rightarrow OH \cdot (\text{hydroxyl radical})$$

These reactions collectively lead to the degradation and decolorization of organic dyes on CuO-NP surface through a series of reduction and oxidation processes.

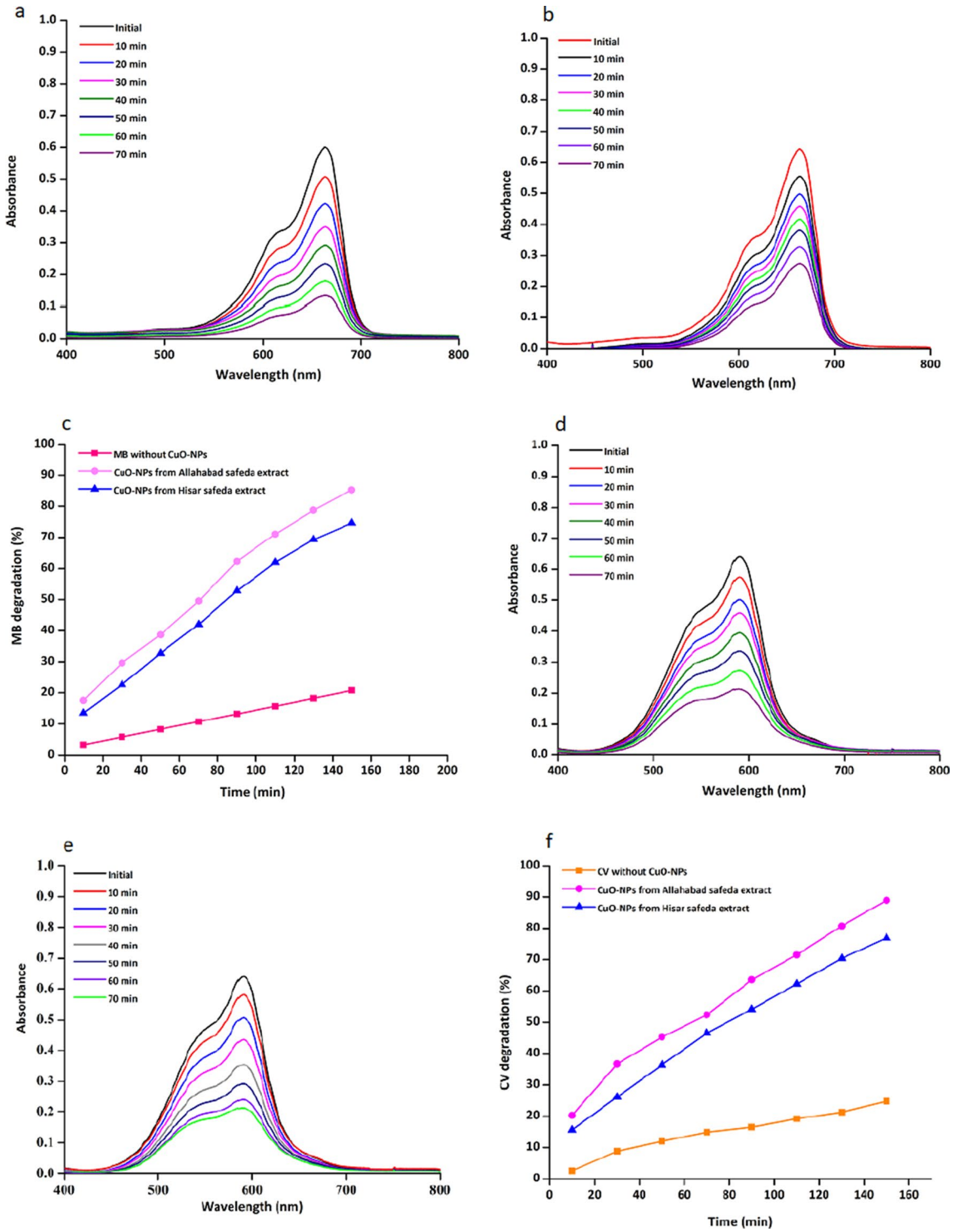

Fig. 5 MB photodegradation by CuO-NPs derived from **a** Allahabad Safeda and **b** Hisar Safeda extracts under UV irradiation, **c** MB photodegradation (%) by CuO-NPs; CV photodegradation by CuO-NPs derived from **d** Allahabad Safeda and **e** Hisar Safeda extracts under UV irradiation, **f** CV photodegradation (%) by CuO-NPs

3.3.7 Role of ROS in photocatalytic dye degradation

The scavenging activity results (Fig. 6) indicate the significant role of scavengers on the photodegradation of dyes (MB and CV) using CuO-NPs derived from Allahabad Safeda and Hisar Safeda extracts. The results revealed the critical role of superoxide and hydroxyl radicals in the photodegradation of both dyes. CuO-NPs from Allahabad Safeda extract presented

Table 4 UV photodegradation kinetics of MB and CV by CuO-NPs synthesized from Allahabad Safeda and Hisar Safeda extracts

Photocatalytic activity		CuO-NPs from Allahabad Safeda			CuO-NPs from Hisar Safeda		
		Degradation (%)	Rate constant (min^{-1})	Regression coefficient (R^2)	Degradation (%)	Rate constant (min^{-1})	Regression coefficient (R^2)
Under UV irradiation	Methylene blue	82.31	0.0691	0.992	72.69	0.0465	0.979
	Crystal violet	88.54	0.0682	0.987	76.78	0.0487	0.986

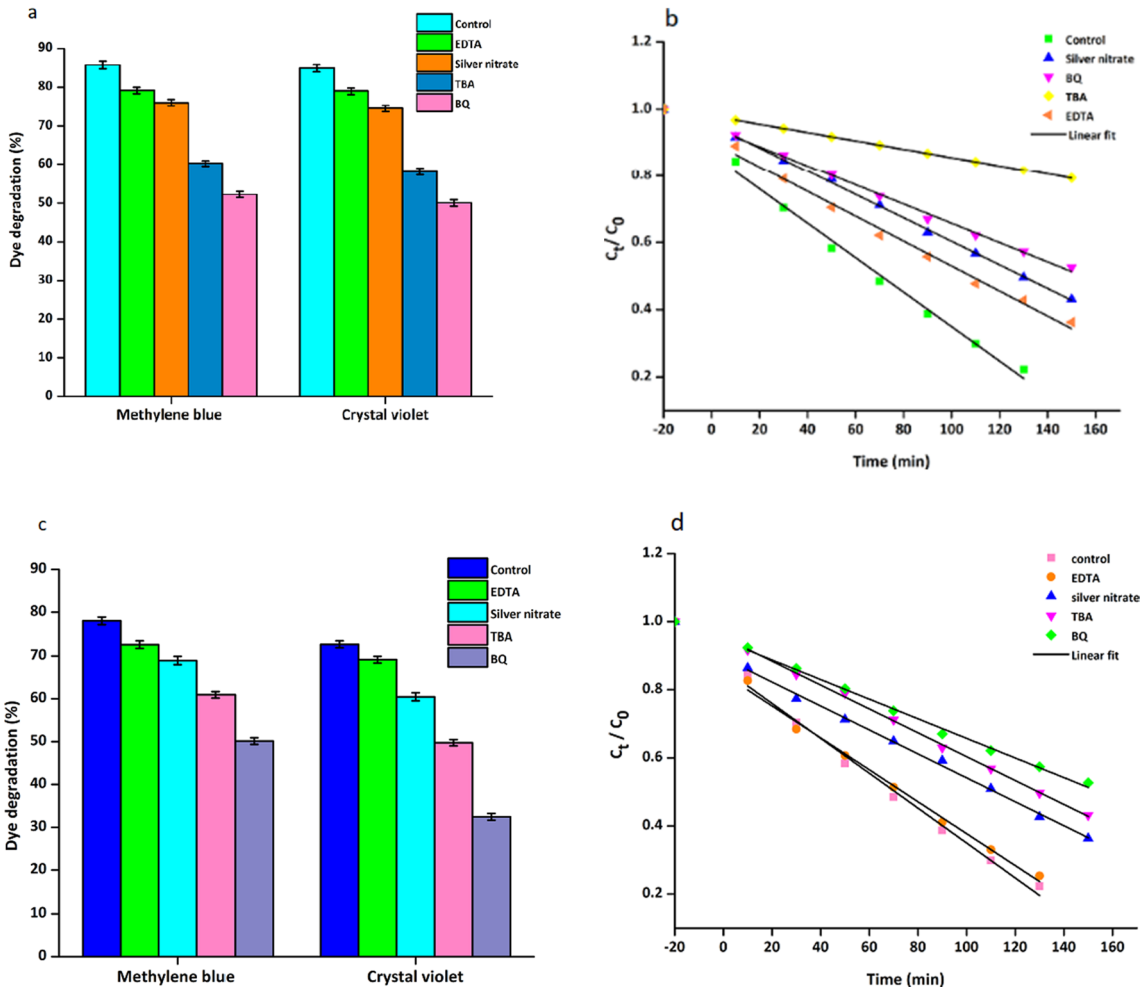

Fig. 6 Impact of scavengers on the photodegradation of dye by CuO-NPs derived from (**a**–**b**) Allahabad Safeda, and (**c**–**d**) Hisar Safeda extracts

degradation rates of 52.31% MB and 50.1% CV dyes when BQ was used as the scavenger. Similarly, in the presence of TBA scavenger, the degradation rate reached 51.23% and 48.23% for MB and CV dyes. In contrast, scavengers such as EDTA and silver nitrate, which scavenge holes and free electrons, had a minor impact on the degradation process (Fig. 6a, b). In the presence of EDTA and silver nitrate scavengers, MB degradation was 79.29% and 75.62% while CV degradation was 77.75% and 74.23%, respectively. On the other hand, using CuO-NPs derived from Hisar Safeda extract, the photodegradation of MB and CV dyes was significantly influenced by the presence of TBA and BQ scavengers (Fig. 6c, d). The utilization of TBA as a scavenger resulted in a degradation rate of 51.32% for MB and 50.61% for CV. Furthermore, in the presence of a BQ scavenger, the degradation rates reached 48.59% MB and 48.99% CV, highlighting the significant role of superoxide free radicals in the photodegradation process. In addition, scavengers like EDTA and silver nitrate had a limited impact on dye photodegradation (Fig. 6c). In the presence of EDTA as a scavenger, MB

and CV photodegradation occurred at 68.21% and 66.32%, while for silver nitrate scavengers, the degradation rates were recorded at 64.32% of MB and 62.12% of CV.

4 Conclusions

This research investigated the utilization of two varieties of *Psidium guajava* (Allahabad Safeda and Hisar Safeda) leaf extracts for the eco-friendly synthesis of CuO-NPs. The bioactive compounds in Allahabad Safeda and Hisar Safeda extracts played a critical role in shaping the nanoparticle formation process. The CuO-NPs synthesized using 3% Allahabad Safeda extract and 7% Hisar Safeda extract generated a particle size of 15.88 nm and 14.05 nm. The functional groups in CuO-NPs were identified through FTIR characterization. Notably, CuO-NPs derived from Allahabad Safeda extract displayed enhanced capabilities than those from Hisar Safeda extract, presenting remarkable antimicrobial activity against bacteria *S. aureus*, *S. lactis*, *E. coli*, and *P. aeruginosa*, with inhibition zones of 20.5 mm, 20.7 mm, 19.5 mm, and 19.7 mm, respectively. Additionally, these nanoparticles displayed significant DPPH scavenging activity (68.23%), indicative of their strong antioxidation properties. CuO-NPs derived from Allahabad Safeda achieved 71.45% inhibition of amylase activity at 100 µg/mL. Furthermore, CuO-NPs derived from Allahabad Safeda exhibited significant photodegradation of MB (82.31%) and CV (88.54%) in 150 min. In summary, the results demonstrated environmentally friendly CuO-NPs synthesis using *Psidium guajava*, which offered promising avenues for novel and sustainable approaches to tackle current global challenges in environmental protection.

Acknowledgements The authors express their gratitude for the continuous research assistance provided by the Faculty of Food Technology and Horticulture at Lovely Professional University, India.

Author contribution Samriti Guleria (S.G.): conceptualization, methodology, investigation, writing—original draft preparation.

Ankush Relhan (A.R.): investigation, data curation, writing—original draft preparation.

Aparajita Bhasin (A.B.): methodology, writing—review and editing.

Anis Mirza (A.M.): conceptualization, methodology, writing—review and editing.

John L. Zhou (J.L.Z.): data curation, writing—review and editing.

Funding Open Access funding enabled and organized by CAUL and its Member Institutions Open access funding is provided by the Library, University of Technology Sydney Library.

Data availability The datasets will be made available upon request.

Declarations

Ethical approval This declaration is not applicable.

Competing interests The authors declare no competing interests.

References

1. Abdullah Rahman AU, Faisal S, Almostafa MM, Younis NS, Yahya G (2023) Multifunctional spirogyra-hyalina-mediated barium oxide nanoparticles (BaONPs): synthesis and applications. Molecules 28(17):6364
2. Al-Radadi NS, Faisal S, Alotaibi A, Ullah R, Hussain T, Rizwan M, Zaman N, Iqbal M, Iqbal A, Ali Z (2022) Zingiber officinale driven bioproduction of ZnO nanoparticles and their anti-inflammatory, anti-diabetic, anti-Alzheimer, anti-oxidant, and anti-microbial applications. Inorg Chem Commun 140:109274
3. Al-Radadi NS, Hussain T, Faisal S, Shah SAR (2022) Novel biosynthesis, characterization and bio-catalytic potential of green algae (*Spirogyra hyalina*) mediated silver nanomaterials. Saudi J Biol Sci 29(1):411–419
4. Belhaj D, Frikha D, Athmouni K, Jerbi B, Ahmed MB, Bouallagui Z, Kallel M, Maalej S, Zhou J, Ayadi H (2017) Box-Behnken design for extraction optimization of crude polysaccharides from Tunisian *Phormidium versicolor* cyanobacteria (NCC 466): partial characterization, in vitro antioxidant and antimicrobial activities. Int J Biol Macromol 105:1501–1510
5. Brasiunas B, Popov A, Ramanavicius A, Ramanaviciene A (2021) Gold nanoparticle-based colorimetric sensing strategy for the determination of reducing sugars. Food Chem 351:129238
6. Caroling G, Priyadharshini MN, Vinodhini E, Ranjitham AM, Shanthi P (2015) Biosynthesis of copper nanoparticles using aqueous guava extract-characterisation and study of antibacterial effects. Int J Pharm Biol 5(2):25–43
7. Chandraker SK, Lal M, Ghosh MK, Tiwari V, Ghorai TK, Shukla R (2020) Green synthesis of copper nanoparticles using leaf extract of *Ageratum houstonianum* Mill. and study of their photocatalytic and antibacterial activities. Nano Express 1(1):010033
8. Karri S, Sharma S, Hatware K, Patil K (2019) Natural anti-obesity agents and their therapeutic role in management of obesity: a future trend perspective. Biomed Pharmacother 110:224–238
9. Chen W, Wu J, Weng X, Owens G, Chen Z (2022) One-step green synthesis of hybrid Fe-Mn nanoparticles: methodology, characterization and mechanism. J Clean Prod 363:132406
10. Kumar M, Kaushik D, Kumar A, Gupta P, Proestos C, Oz E, Orphan E, Kaur J, Khan MR, Elobeid T, Bordia M, Oz F (2023) Green synthesis of copper nanoparticles from Nigella sativa seed extract and evaluation of their antibacterial and antiobesity activity. Int J Food Sci Technol 58(6):2883–2892
11. Chinnathambi A, Awad Alahmadi T, Ali Alharbi S (2021) Biogenesis of copper nanoparticles (Cu-NPs) using leaf extract of *Allium noeanum*, antioxidant and in-vitro cytotoxicity. Artif Cells Nanomed Biotechnol 49(1):500–510

12. Xu C, Liang Z, Tang D, Xiao T, Tsunoda M, Zhang Y, ... & Song Y (2017) Gas chromatography-mass spectrometry (GC-MS) analysis of volatile components from guava leaves. J Essent Oil Bear Plants 20(6):1536–1546
13. Dabhane H, Ghotekar S, Zate M, Lin KYA, Rahdar A, Ravindran B, Bahiram D, Ingale C, Khairnar B, Sali D, Kute S (2023) A novel approach toward the bio-inspired synthesis of CuO nanoparticles for phenol degradation and antimicrobial applications. Biomass Convers Biorefin. https://doi.org/10.1007/s13399-023-03954-y
14. Faisal S, Jan H, Abdullah Alam I, Rizwan M, Hussain Z ... Uddin MN (2022). In vivo analgesic, anti-inflammatory, and anti-diabetic screening of Bacopa monnieri-synthesized copper oxide nanoparticles. ACS Omega 7(5):4071–4082
15. Khan MA, Ali F, Faisal S, Rizwan M, Hussain Z, Zaman N, Afsheen Z, Uddin MN, Bibi N (2021) Exploring the therapeutic potential of Hibiscus rosa sinensis synthesized cobalt oxide (Co3O4-NPs) and magnesium oxide nanoparticles (MgO-NPs). Saudi J Biol Sci 28(9):5157–5167
16. Imran M, Jan H, Faisal S, Shah SA, Shah S, Khan MN ... Syed S (2021) In vitro examination of anti-parasitic, anti-Alzheimer, insecticidal and cytotoxic potential of Ajuga bracteosa Wallich leaves extracts. Saudi J Biol Sci 28(5):3031–3036
17. de Oliveira GT, Possolli NM, Polla MB, Wermuth TB, de Oliveira TF, Eller S, Montedo ORK, Arcaro S, Cechinel MAP (2021) Photocatalytic pathway on the degradation of methylene blue from aqueous solutions using magnetite nanoparticles. J Clean Prod 318:128556
18. Kumar M, Kapoor S, Dhumal S, Tkaczewska J, Changan S, Saurabh V, Radha MM, Rais N, Satankar V, Pandiselvam R, Sayed AAS, Sanpathy M, Anitha A, Singh S, Tomar M, Dey A, Zengin G, Amaroicz R, Bhuyan DJ (2022) Guava (Psidium guajava L.) seed: A low-volume, high-value byproduct for human health and the food industry. Food Chem 386:132694
19. DeFronzo RA, Ferrannini E, Groop L, Henry RR, Herman WH, Holst JJ, Weiss R (2015) Type 2 diabetes mellitus. Nat Rev Dis Primers 1(1):1–22
20. Díaz-de-Cerio E, Gómez-Caravaca AM, Verardo V, Fernández-Gutiérrez A, Segura-Carretero A (2016) Determination of guava (Psidium guajava L.) leaf phenolic compounds using HPLC-DAD-QTOF-MS. J Funct Foods 22:376–388
21. Dinh TA, Le YN, Pham NQ, Ton-That P, Van-Xuan T, Ho TGT, Phuong HHK (2023) Fabrication of antimicrobial edible films from chitosan incorporated with guava leaf extract. Prog Org Coat 183:107772
22. Eze FN, Ovatlarnporn C, Nalinbenjapun S, Sripetthong S (2022) Ultra-fast sustainable synthesis, optimization and characterization of guava phenolic extract functionalized nanosilver with enhanced biomimetic attributes. Arab J Chem 15(10):104167
23. Jan H, Shah M, Andleeb A, Faisal S, Khattak A, Rizwa, M,... Abbasi BH (2021) Plant-based synthesis of zinc oxide nanoparticles (ZnO-NPs) using aqueous leaf extract of aquilegia pubiflora: their antiproliferative activity against HepG2 cells inducing reactive oxygen species and other in vitro properties. Oxid Med Cell Longev 2021
24. Faisal S, Abdullah, Jan H, Shah SA, Shah S, Rizwan M, ... & Masood R (2021) Bio-catalytic activity of novel Mentha arvensis intervened biocompatible magnesium oxide nanomaterials. Catalysts 11(7):780
25. Faisal S, Al-Radadi NS, Jan H, Abdullah, Shah SA, Shah S, ... & Bibi N (2021) Curcuma longa mediated synthesis of copper oxide, nickel oxide and Cu-Ni bimetallic hybrid nanoparticles: characterization and evaluation for antimicrobial, anti-parasitic and cytotoxic potentials. Coatings 11(7):849
26. Saeedi P, Petersohn I, Salpea P, Malanda B, Karuranga S, Unwin N, Colagiuri S, Guariguata L, Motala AA, Ogurtsova K, Shaw JE (2019) Global and regional diabetes prevalence estimates for 2019 and projections for 2030 and 2045: results from the international diabetes federation diabetes atlas. Diabetes Res Clin Pract 157:107843
27. Faisal S, Jan H, Shah SA, Shah S, Khan A, Akbar MT, ... & Syed S (2021) Green synthesis of zinc oxide (ZnO) nanoparticles using aqueous fruit extracts of Myristica fragrans: their characterizations and biological and environmental applications. ACS omega 6(14):9709–9722
28. Faisal S, Khan MA, Jan H, Shah SA, Shah S, Rizwan M, Akbar MT (2020) Edible mushroom (*Flammulina velutipes*) as biosource for silver nanoparticles: from synthesis to diverse biomedical and environmental applications. Nanotechnology 32(6):065101
29. Faisal S, Rizwan M, Ullah R, Alotaibi A, Khattak A, Bibi N, Idrees M (2022) Paraclostridium benzoelyticum bacterium-mediated zinc oxide nanoparticles and their in vivo multiple biological applications. Oxid Med Cell Longev 2022
30. Faisal S, Tariq MH, Ullah R, Zafar S, Rizwan M, Bibi N, ... & Abdullah (2023) Exploring the antibacterial, antidiabetic, and anticancer potential of Mentha arvensis extract through in-silico and in-vitro analysis. BMC Complementary Med Ther 23(1):267
31. Faisal S, Ullah R, Alotaibi A, Zafar S, Rizwan M, Tariq MH (2023) Biofabrication of silver nanoparticles employing biomolecules of Paraclostridium benzoelyticum strain: Its characterization and their in-vitro antibacterial, anti-aging, anti-cancer and other biomedical applications. Microsc Res Tech 86(7):846–861
32. Kumar M, Tomar M, Amarowicz R, Saurabh V, Nair MS, Maheshwari C, Sasi S, Prajapati U, Hasan M, Singh S, Changan S, Prajapat RK, Berwal MK, Satankar V (2021) Guava (Psidium guajava L.) leaves: Nutritional composition, phytochemical profile, and health-promoting bioactivities. Foods 10(4):752
33. Zafar S, Faisal S, Jan H, Ullah R, Rizwan M, Abdullah … Khattak A, (2022) Development of iron nanoparticles (FeNPs) using biomass of enterobacter: its characterization, antimicrobial, anti-Alzheimer's, and enzyme inhibition potential. Micromachines 13(8):1259
34. Rizwan M, Faisal S, Tariq MH, Zafar S, Khan A, Ahmad F (2023) Enterobacter hormaechei-driven novel biosynthesis of tin oxide nanoparticles and evaluation of their anti-aging, cytotoxic, and enzyme inhibition potential. ACS Omega 8(30):27439–27449
35. Varympopi A, Dimopoulou A, Papafotis D, Avramidis P, Sarris I, Karamanidou T, ... & Skandalis N (2022) Antibacterial activity of copper nanoparticles against Xanthomonas campestris pv. vesicatoria in tomato plants. Int J Mol Sci 23(8):4080
36. Wang L, Lu F, Liu Y, Wu Y, Wu Z (2018) Photocatalytic degradation of organic dyes and antimicrobial activity of silver nanoparticles fast synthesized by flavonoids fraction of *Psidium guajava* L. leaves. J Mol Liq 263:187–192
37. Gaber SE, Hashem AH, El-Sayyad GS, Attia MS (2023) Antifungal activity of myco-synthesized bimetallic ZnO-CuO nanoparticles against fungal plant pathogen Fusarium oxysporum. Biomass Convers Biorefin. https://doi.org/10.1007/s13399-023-04550-w
38. Ghosh MK, Sahu S, Gupta I, Ghorai TK (2020) Green synthesis of copper nanoparticles from an extract of *Jatropha curcas* leaves: Characterization, optical properties, CT-DNA binding and photocatalytic activity. RSC Adv 10(37):22027–22035
39. Guleria S, Simsek H, Chawla P, Relhan A, Bhasin A (2023) Evaluation of Cladophora and Chlamydomonas microalgae for environmental sustainability: a comparative study of antimicrobial and photocatalytic dye degradation. Environ Pollut 340:122806
40. Hussain T, Faisal S, Rizwan M, Zaman N, Iqbal M, Iqbal A, Ali Z (2022) Green synthesis and characterization of copper and nickel hybrid nanomaterials: investigation of their biological and photocatalytic potential for the removal of organic crystal violet dye. J Saudi Chem Soc 26(4):101486
41. Nagaraja S, Ahmed SS, DR B, Goudanavar P, Fattepur S, Meravanige G, ... & Telsang M (2022) Green synthesis and

characterization of silver nanoparticles of Psidium guajava leaf extract and evaluation for its antidiabetic activity. Molecules 27(14):4336
42. Zafar I, Hussain AI, Fatima T, Abdullah Alnasser SM, Ahmad A (2022) Inter-varietal variation in phenolic profile, sugar contents, antioxidant, anti-proliferative and antibacterial activities of selected Brassica species. Appl Sci 12(12):5811
43. Khan MI, Shah S, Faisal S, Gul S, Khan S, Abdullah ... & Shah WA (2022) Monotheca buxifolia driven synthesis of zinc oxide nano material its characterization and biomedical applications. Micromachines 13(5):668
44. Xu B, Ahmed MB, Zhou JL, Altaee A (2020) Visible and UV photocatalysis of aqueous perfluorooctanoic acid by TiO_2 and peroxymonosulfate: process kinetics and mechanistic insights. Chemosphere 243:125366
45. Kaningini AG, Motlhalamme T, More GK, Mohale KC, Maaza M (2023) Antimicrobial, antioxidant, and cytotoxic properties of biosynthesized copper oxide nanoparticles (CuO-NPs) using Athrixia phylicoides DC. Heliyon 9(4):15265
46. Muthukumar H, Matheswaran M (2015) *Amaranthus spinosus* leaf extract mediated FeO nanoparticles: physicochemical traits, photocatalytic and antioxidant activity. ACS Sustain Chem Eng 3(12):3149–3156
47. Navidpour AH, Abbasi S, Li D, Mojiri A, Zhou JL (2023) Investigation of advanced oxidation process in the presence of TiO_2 semiconductor as photocatalyst: property, principle, kinetic analysis, and photocatalytic activity. Catalysts 13(2):232
48. Nguyen DK, Hung NQ, Dinh VP (2023) Antibacterial properties of silver nanoparticles greenly synthesized using guava fruit extract as a reducing agent and stabilizer. Appl Nanosci 13(6):3709–3720
49. Hassan EM, El Gendy AEN G, Abd-ElGawad AM, Elshamy AI, Farag MA, Islam MJ, Khatun N, Bhuiyan RH, Sultana S, Shaikh MAA, Bitu MNA ... Islam S (2023) Psidium guajava leaf extract mediated green synthesis of silver nanoparticles and its application in antibacterial coatings. RSC Adv 13(28):19164–19172
50. Mahmoud AED, El-Maghrabi N, Hosny M, Fawzy M (2022) Biogenic synthesis of reduced graphene oxide from Ziziphus spina-christi (Christ's thorn jujube) extracts for catalytic, antimicrobial, and antioxidant potentialities. Environ Sci Pollut Res 29(59):89772–89787
51. Ullah R, Shah S, Muhammad Z, Shah SA, Faisal S, Khattak U, ... & Taj Akbar M (2021) In vitro and in vivo applications of Euphorbia wallichii shoot extract-mediated gold nanospheres. Green Processing and Synthesis 10(1):101–111
52. Mali SC, Dhaka A, Githala CK, Trivedi R (2020) Green synthesis of copper nanoparticles using *Celastrus paniculatus* Willd. leaf extract and their photocatalytic and antifungal properties. Biotechnol Rep 27:e00518
53. Ntoumba AA, Meva FEA, Ekoko WE, Foko LPK, Hondt EN, Schlüsener C, ... & Lehman LG (2019) Biogenic synthesis of silver nanoparticles using guava (Psidium guajava) leaf extract and its larvicidal action against Anopheles gambiae. J Biomaterials and Nanobiotechnology 11(01):49
54. Sathiyavimal S, Vasantharaj S, Veeramani V, Saravanan M, Rajalakshmi G, Kaliannan T, ... & Pugazhendhi A (2021) Green chemistry route of biosynthesized copper oxide nanoparticles using Psidium guajava leaf extract and their antibacterial activity and effective removal of industrial dyes. J Environ Chem Eng 9(2):105033
55. Mahmoud NM, Al-Otaibi AL, Akhtar S, Ansari MA, Ramadan A, Ahmed SB (2023) Study the effect of simple extraction techniques to synthesizing promising antimicrobial bio-capped copper oxide nanoparticles. Green Chem Lett Rev 16(1):2260417
56. Kaningini AG, Motlhalamme T, More GK, Mohale KC, Maaza M (2023) Antimicrobial, antioxidant, and cytotoxic properties of biosynthesized copper oxide nanoparticles (CuO-NPs) using Athrixia phylicoides DC. Heliyon 9(4):e15265
57. Peddi P, Ptsrk PR, Rani NU, Tulasi SL (2021) Green synthesis, characterization, antioxidant, antibacterial, and photocatalytic activity of Suaeda maritima (L.) Dumort aqueous extract-mediated copper oxide nanoparticles. J Genetic Eng Biotechnol 19(1):1–11
58. Rehana D, Mahendiran D, Kumar RS, Rahiman AK (2017) Evaluation of antioxidant and anticancer activity of copper oxide nanoparticles synthesized using medicinally important plant extracts. Biomed Pharmacother 89:1067–1077
59. Mahmoud M, Mohamed EM, Aboul-Enein AM, Diab AA, Shalaby EA (2023) Anticancer and antioxidant activities of ethanolic extract and semi-purified fractions from guava and mango seeds. Biomass Convers Biorefin. https://doi.org/10.1007/s13399-023-04216-7
60. Shah S, Shah SA, Faisal S, Khan A, Ullah R, Ali N, Bilal M (2022) Engineering novel gold nanoparticles using Sageretia thea leaf extract and evaluation of their biological activities. J Nanostruct Chem 12(1):129–140
61. Kokilananthan S, Bulugahapitiya VP, Manawadu H, Gangabadage CS (2022) Sesquiterpenes and monoterpenes from different varieties of guava leaf essential oils and their antioxidant potential. Heliyon 8(12):e12104
62. Peddi P, Ptsrk PR, Rani NU, Tulasi SL (2021) Green synthesis, characterization, antioxidant, antibacterial, and photocatalytic activity of *Suaeda maritima* (L.) Dumort aqueous extract-mediated copper oxide nanoparticles. J Genetic Eng Biotechnol 19(1):131
63. Luque-Jacobo CM, Cespedes-Loayza AL, Echegaray-Ugarte TS, Cruz-Loayza JL, Cruz I, de Carvalho JC, Goyzueta-Mamani LD (2023) Biogenic synthesis of copper nanoparticles: a systematic review of their features and main applications. Molecules 28(12):4838
64. Khadayat K, Marasini BP, Gautam H, Ghaju S, Parajuli N (2020) Evaluation of the alpha-amylase inhibitory activity of Nepalese medicinal plants used in the treatment of diabetes mellitus. Clin Phytosci 6(1):1–8
65. Sibhatu AK, Weldegebrieal GK, Sagadevan S, Tran NN, Hessel V (2022) Photocatalytic activity of CuO nanoparticles for organic and inorganic pollutants removal in wastewater remediation. Chemosphere 300:134623
66. Vishnu G, Singh S, Naik TSK, Viswanath R, Ramamurthy PC, Bhadrecha P, ... & Zahmatkesh S (2023) Photodegradation of methylene blue dye using light driven photocatalyst-green cobalt doped cadmium ferrite nanoparticles as antibacterial agents. J Cleaner Prod 404:136977
67. Hamami Z, Javanbakht V (2023) Photocatalytic processes using potato peel extract-mediated CuO nanophotocatalyst for fast and efficient direct red 80 dye removal. Biomass Convers Biorefin. https://doi.org/10.1007/s13399-023-05034-7
68. Kumar M, Mehta A, Mishra A, Singh J, Rawat M, Basu S (2018) Biosynthesis of tin oxide nanoparticles using *Psidium Guajava* leave extract for photocatalytic dye degradation under sunlight. Mater Lett 215:121–124
69. Rezaie AB, Montazer M, Rad MM (2018) Environmentally friendly low-cost approach for nano copper oxide functionalization of cotton designed for antibacterial and photocatalytic applications. J Clean Prod 204:425–436
70. Sougandhi PR, Ramanaiah S (2020) Green synthesis and spectral characterization of silver nanoparticles from Psidium guajava leaf extract. Inorg Nano-Met Chem 50(12):1290–1294
71. Varughese A, Kaur R, Singh P (2020) Green synthesis and characterization of copper oxide nanoparticles using Psidium guajava leaf extract. In IOP Conference Series: Materials Science and Engineering, Vol. 961. IOP Publishing, No. 1, p 012011

72. Selvam K, Albasher G, Alamri O, Sudhakar C, Selvankumar T, Vijayalakshmi S, Vennila L (2022) Enhanced photocatalytic activity of novel *Canthium coromandelicum* leaves based copper oxide nanoparticles for the degradation of textile dyes. Environ Res 211:113046
73. Wardani M, Yulizar Y, Abdullah I, & Bagus Apriandanu DO (2019) Synthesis of NiO nanoparticles via green route using Ageratum conyzoides L. leaf extract and their catalytic activity. In IOP Conference Series: Materials Science and Engineering, Vol. 509. IOP Publishing, p 012077